WIN55212-2 Docking to the CB_1 Cannabinoid Receptor and Multiple Pathways for Conformational Induction

Joong-Youn Shim* and Allyn C. Howlett

Neuroscience of Drug Abuse Research Program, J. L. Chambers Biomedical/Biotechnology Research Institute, North Carolina Central University, Durham, North Carolina 27707

Received November 3, 2005

Key pharmacophoric elements for the (aminoalkyl)indole (AAI) CB_1 cannabinoid receptor agonists are the aminoalkyl moiety, the lipophilic aroyl group, and the heterocyclic indole ring. In the present study, the docking space allowed for (*R*)-[2,3-dihydro-5-methyl-3-[(4-morpholinyl)methyl]pyrrolo[1,2,3-*de*]-1,4-benzoxazin-6-yl](1-naphthalenyl)methanone (WIN55212-2; **1**) within the CB_1 receptor was extensively explored by a docking approach that combines Monte Carlo (MC) and molecular dynamics (MD) simulations. The goals were to understand the key binding interactions of AAIs within the CB_1 receptor and to examine the role of the ligand in inducing a receptor conformational change. From the findings of extensive SAR studies on the cannabinoid compounds and correlation between AAI binding affinity data and calculated binding energies, we proposed two alternative binding conformations, *aroyl-up1* and *aroyl-up2*. These denote the directionality of the ligand naphthyl ring within the receptor upward with respect to the extracellular side. A comprehensive structural analysis of **1** demonstrated that the aroyl ring moiety could be important as the steric trigger for inducing CB_1 receptor conformational change. Thus, it appears that aromatic−aromatic interactions are important not only for the binding of **1** but also for inducing receptor conformational change. It is possible that differences in the nature of the ligand binding could contribute to ligand-specific conformational changes in the receptor.

INTRODUCTION

Cannabinoid (CB) receptors are G-protein-coupled receptors (GPCRs) that have a common core structure composed of seven transmembrane (TM) helices (TM1−TM7) connected by three extracellular (E1, E2, and E3) and three intracellular (I1, I2, and I3) loops, and belong to the rhodopsin/β2 adrenergic receptor-like subfamily.[1] Two subtypes of the CB receptors have been identified: brain CB_1[2,3] and immune CB_2[4] receptors. Multiple chemical classes of CB_1 receptor agonists are known,[5] including) the following: (i) classical and nonclassical cannabinoid analogues, typified by 4-[4-(1,1-dimethylheptyl)-2-hydroxyphenyl]perhydro-2α,6β-dihydroxynaphthalene (CP55244; **2**) and Δ^9-tetrahydrocannabinol (Δ^9-THC; **3**), respectively; (ii) (aminoalkyl)-indole (AAI) analogues, typified by **1**; and (iii) eicosanoid cannabimimetic compounds, typified by arachidonylethanolamide (anandamide; **4**) (Figure 1).

In response to ligand binding, GPCRs change their conformations to activate the associated G-proteins.[1] Two ligand-mediated GPCR activation models have been proposed: the conformation selection model and the ligand induction model. In the conformational selection model,[6] agonists preferentially bind to (and stabilize) the receptor in the R* (active) conformation over the receptor in R (inactive) conformation, thereby increasing the duration of time that the receptor remains in the R* state. In contrast, according to the ligand induction model,[7] ligands initially bind to the R state and induce a conformational change to the R* state.

* Corresponding author phone: (919)530-7763; fax: (919)530-7760; e-mail: jyshim@nccu.edu.

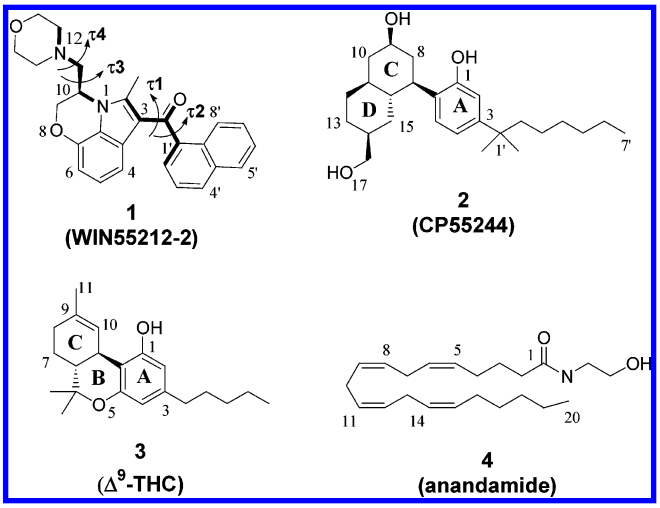

Figure 1. Molecular structures of CB_1 receptor ligands.

Binding of agonist ligands to CB_1 receptors stimulates G-proteins for signal transduction pathways that inhibit adenylyl cyclase activity and regulate ion channels.[8] The structure−activity relationships (SAR) for the CB_1 receptor have been extensively studied. To understand the SAR at the molecular level, it is necessary to determine the ligand bound-CB_1 receptor structure that can reveal key binding interactions between the ligand and the binding site residues. From recent mutation studies on the human CB_1 cannabinoid receptor,[9,10] it was shown that the K3.28(192) mutations to Ala, Gln, or Glu resulted in a significant loss of binding for classical and nonclassical cannabinoid ligands and anandamide but not for **1**. Because it is known from the SAR

10.1021/ci0504824 CCC: $33.50
Published on Web 02/21/2006

studies of cannabinoids that the A-ring OH is one of the key pharmacophoric elements, this moiety of the classical and nonclassical cannabinoids has been proposed to form a H-bond with the side chain of K192.[9−11] Among several reported docking models of the cannabinoids, the models by Shim and colleagues[12] for the CB_1 receptor and Tao and colleagues[13] for the CB_2 receptor employed this H-bond as the key constraint to position their cannabinoid ligands.

From SAR studies on AAI compounds,[14−18] the key pharmacophoric elements were the aminoalkyl moiety, the lipophilic aroyl group, and the heterocyclic indole ring. Cannabinoid and AAI ligands are believed to share a common binding region as inferred from the competitive displacement of [^{3}H]CP55940 by the AAIs[17,18] and of [^{3}H]WIN55212-2 by the cannabinoid compounds.[16,19] On the premise that aromatic stacking interactions play a major role in binding of AAIs to the CB_1 receptor and in subsequent receptor activation, Song and colleagues[20] used a set of aromatic residues, F3.25(189), F3.36(200), W(255), and W5.43(279), forming a cluster according to their receptor model,[21] as an anchor point for the naphthyl ring moiety for the docking of **1**. In the same study, it was reported that the mutation of the CB_1 receptor V5.46(282) to Phe resulted in a moderate increase (13-fold) in the binding affinity of **1**. However, it is not clear whether this residue interacts directly with **1** or indirectly by modulating interaction with other receptor residues for tighter ligand binding. Recently, McAllister et al.[22] reported a binding conformation of **1** in an active state model of the CB_1 receptor, where the naphthyl ring moiety interacted with F3.36(200), W5.43(279), and W6.48(356), and the indole ring moiety interacted with Y5.39(275). It was shown that mutations of these residues resulted in 3−16-fold decreases in the ligand binding affinity, suggesting that these residues might be involved in **1** binding. Although this study reported that these aromatic residues interacted with the naphthyl or indole ring moiety of the ligand through π-stacking interactions, other receptor intrahelical residues that might be important for **1** binding were not explored. It was noticed that, albeit in different receptor structural models, the binding conformations of **1** by Song et al.[20] and by McAllister et al.[22] were quite dissimilar. Consequently, it was felt that the binding conformation of AAI compounds warranted further investigation and evaluation.

In the present study, we extensively explored the ground-state receptor-bound conformation of **1** and identified key binding interactions of AAIs with the receptor. A working assumption was that **1** shares the same hydrophobic pocket that has been proposed to interact with the C3 side chain of cannabinoids, a crucial pharmacophore for the CB_1 receptor binding and activation.[23−30] It appears that aromatic−aromatic interactions are important not only for the binding of **1** but also for inducing receptor conformational change. The present results suggest that variations in the receptor−ligand interactions by structurally different ligands would initiate different types of receptor motions for agonist-specific conformational changes in the receptor.

COMPUTATIONAL METHODS

All the calculations were performed on a Silicon Graphics Origin2000 workstation. Molecular docking simulations were carried out using the consistent force field (CFF)[31] implemented in *InsightII* (Accelrys, Inc. San Diego, CA). CFF is a second-generation force field that is able to accurately predict the geometry and energetics of a large number of classes of compounds. For energy minimizations, the steepest descent method was applied first to a 100 kcal/mol·Å energy gradient followed by the Polak and Ribiere conjugate gradients method[32] until the final convergence criterion of 0.01 kcal/mol·Å energy gradient was achieved. The cell multipole method[33] with a distance-dependent dielectric constant ($\epsilon = \epsilon_0 r$, with $\epsilon_0 = 4.0$) was used for summation of nonbonding interactions.

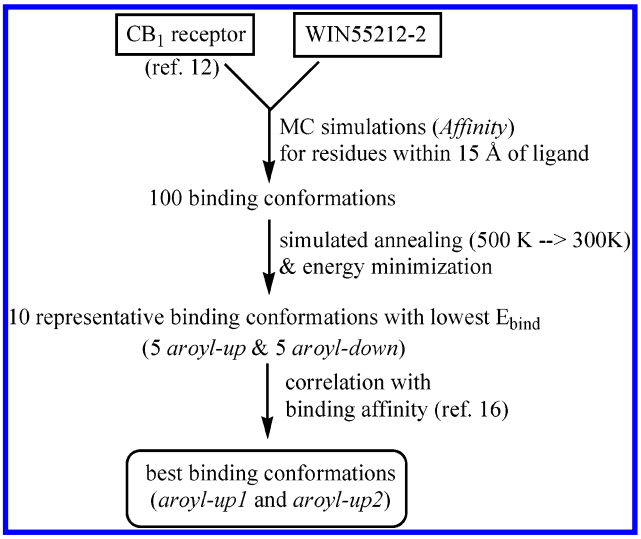

Figure 2. A flow diagram of the computational approaches to determine the **1** binding conformations to the CB_1 receptor.

A flow diagram of the computational approaches employed in the present docking study is shown in Figure 2. A combination of Monte Carlo (MC) and molecular dynamics (MD) simulation approaches was used to identify the binding conformations of **1**. For the receptor structure, the CB_1 receptor homology model[12] that was constructed using the published X-ray crystal structure of bovine rhodopsin[34] was used. For the ligand **1** structure, an initial structure of **1** was built by the *Builder* module in *InsightII*. Based upon the measured pK_a value of 5.0−5.3 (25 °C) for pravadoline,[15] the morpholine N of **1** would exist largely unprotonated at physiological pH. Thus, **1** with the morpholine N being unprotonated was considered in this study. Among three binding pockets (defined as P1, P2, and P3) of the CB_1 receptor from the previously identified binding conformation of **2**,[12] the P1 pocket corresponded to the hydrophobic pocket (Figure 3A) that interacts with the C3 side chain of **2**.[12] The binding conformation of **2** within the receptor binding pocket was replaced by **1**, and all the residues within 15 Å of **1** were defined as the binding region. Then, a MC simulation was performed to explore docking conformations of **1** using the *Affinity* module in *InsightII*. During this procedure, the ligand and the side chains of the residues within the defined binding site were allowed to rotate freely, while the TM backbone was restricted. A set of 100 conformations obtained from the MC sampling was subjected to simulated annealing, starting at a temperature of 500 K and then cooling to a temperature of 300 K in 10 ps. Each conformation was then energy-minimized. The selection criterion for choosing the representative binding conformations was that the hydro-

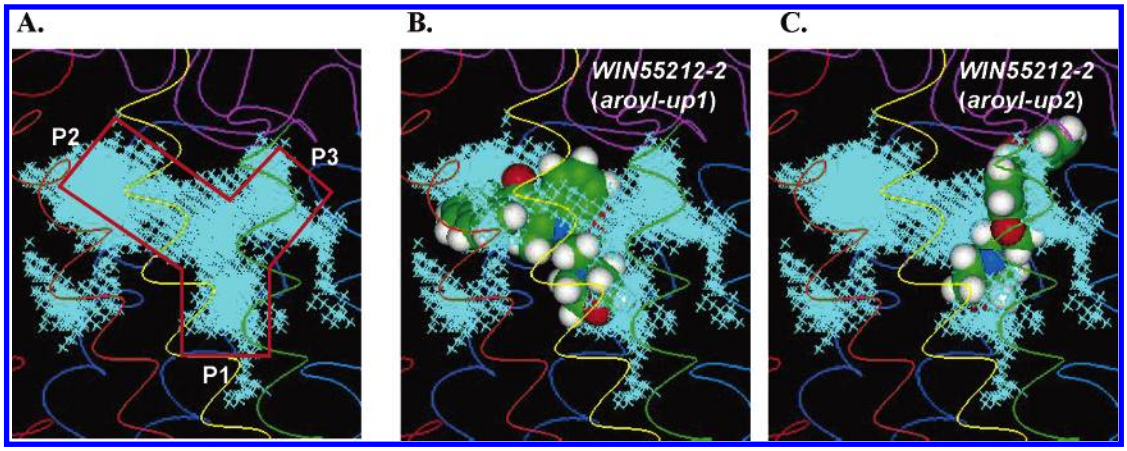

Figure 3. A. The available space for the CB_1 receptor ligand binding within the receptor TM core region identified from the previous docking study of nonclassical ACD-tricyclic cannabinoids.[12] B. The same space for the CB_1 receptor ligand binding occupied by **1** in its *aroyl-up1* binding conformation. C. The same space for the CB_1 receptor ligand binding occupied by **1** in its *aroyl-up2* binding conformation. Binding space is represented as cyan x's as viewed from the membrane side facing TM3. Three assigned ligand binding pockets, P1, P2, and P3, are represented in a Y-shaped polyhedron. The CB_1 receptor helical backbone is represented in ribbon format. TM1−TM7 are colored in red, orange, yellow, green, cyan, blue, and purple, and the extracellular loops are colored in magenta. The binding pocket P1[12] corresponds to a proposed hydrophobic pocket[20−26] that interacts with the C3 alkyl side chain of nonclassical cannabinoid drugs.

phobic pocket that has been proposed to interact with the C3 side chain of cannabinoids[23−29] must be occupied by a moiety of **1**. Ten representative binding conformations of **1** with the lowest ΔE_{bind} were selected. These binding conformations were evaluated by correlating the binding affinity with the calculated ΔE_{bind} for a series of 37 AAIs (i.e., compounds **5**−**41**), having a wide range of affinities for the CB_1 receptor (Table 1), chosen from the study reported by Eissenstat et al.[16] It should be noted that radioligand binding assays from this study were performed under assay conditions that would favor the "ground state" of the receptor (i.e., in the absence of Na^+ or guanine nucleotides). The binding energy (ΔE_{bind}) values for each receptor−ligand complex were calculated, as in our previous study.[12] Making the reasonable assumption that differences in entropic and solvation/desolvation terms will be small within a series of structurally similar ligands, the binding free energy (ΔG_{bind}) was approximated by

$$\Delta G_{bind} \cong \Delta E_{bind} = E_{complex} - (E_{receptor,free} + E_{ligand,free})$$

where ΔE_{bind} is the ligand−receptor interaction energy, $E_{complex}$ is the energy of the ligand−receptor complex, and $E_{receptor,free}$ and $E_{ligand,free}$ are the energies of the receptor and the ligand in the free unbound state.

For conformational analysis, rotational energy barrier calculations, and MD simulations of **1**, the MMFF force field[35] was used, for this force field is known to be suitable for calculating small molecules requiring high accuracy. Conformational analysis of **1** was performed by two different methods, a MC search and a systematic search implemented in *Spartan*'02 (Wavefunction, Inc. Irvine, CA). The MC search involved a simulated annealing by heating the system up to 5000 K. For the systematic search, all the rotatable torsion angles (see below for the definition of the torsion angles) were searched by a 12-fold rotation. Rotational energy barrier calculations were performed using the molecular mechanics MMFF94, semiempirical AM1,[36] and ab initio HF/3-21G(*)[37] methods implemented in *Spartan*'02, using the lowest energy conformation of **1** from the conformational analysis. For the MMFF94 and AM1 calculations, all the structural elements were fully optimized except the torsion angle selected as the torsional driver. For the HF/3-21G(*) calculations, a single point energy at the MMFF-optimized geometries was calculated. A torsion angle driver was taken in 10° increments for the range of 360° (i.e., 36 increments) as the function of the individual torsion angles.

MD simulations of **1** were performed using MMFF94 implemented in *SYBYL* (version 7.0) (Tripos, Inc., St. Louis, MO). After extracting the ligand from the receptor−ligand complex structure within the CB_1 receptor binding pocket,[12] this binding conformation of **1** was subjected to a MD simulation (NVT, canonical ensemble) of 35 ns at 300 K. An implicit solvation model with a distance-dependent dielectric constant of 4 was used to approximate the hydrophobic binding pocket environment. The nonbonded lists were generated using a 12 Å nonbonded cutoff distance and updated every 25 fs. The temperature was controlled by direct scaling of velocities, and the equations of motion were integrated by the Verlet velocity method.[38,39] Thirty-five thousand structures were extracted from the trajectories by sampling every 1 ps. These structures, which represent conformational changes in the initial receptor-bound form with time, were used to analyze the individual torsion angles and characterize conformational properties.

RESULTS

Binding Conformations of 1. The space available to be occupied by small molecule ligands within the CB_1 receptor 7-TM helical structure has been defined and can be identified as three connected pockets (Figure 3A). Occupancy of this space by the nonclassical ACD-tricyclic cannabinoids was analyzed previously,[12] and a receptor−ligand model was verified by correlation of predicted binding energies with experimentally derived thermodynamic affinity constants. This model defined a pocket for the relatively hydrophilic and polar moieties to form hydrogen bonding and van der Waals interactions with helical residues.[12,30] A hydrophobic pocket (P1) was occupied by the hydrophobic C3 alkyl side chain, which could serve as a trigger for activation.[12,30] Our working hypothesis for the AAI ligand docking was that the

Table 1. Corresponding Values of the Experimental CB_1 Receptor Binding Affinity (IC_{50} in nM) and Calculated Binding Energy (ΔE_{bind} in kcal/mol) for 37 AAI Analogues from the Study by Eissenstat et al.[16]

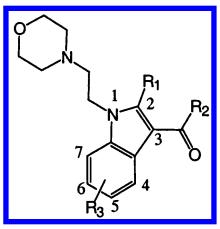

				binding affinity, nM		binding energy, kcal/mol ΔE_{bind}	
	R_1	R_2	R_3	R_1	R_2	aroyl-up1	aroyl-up2
5	H	*p*-OCH_3Ph[b]	H	390	2.59	−47.8	−46.5
6	H	7-benzofuryl	H	18	1.26	−48.3	−49.1
7	H	1-naphthyl	H	7.8	0.89	−52.9	−51.1
8	CH_3	1-naphthyl	H	19	1.28	−52.5	−51.7
9	CH_3	*o*-OCH_3Ph	H	800	2.90	−48.9	−49.2
10	CH_3	*p*-OCH_3Ph	H	3155	3.50	−46.8	−47.1
11	CH_3	*p*-OCH_3Ph	6-CH_3	1883	3.27	−46.4	−48.6
12	CH_3	*p*-OCH_3Ph	7-CH_3	1533	3.19	−48.3	−47.2
13	CH_3	*p*-OCH_3Ph	6-OCH_3	1451	3.16	−51.0	−51.5
14	CH_3	*p*-OCH_3Ph	7-F	571	2.76	−47.4	−46.2
15	CH_3	*p*-OCH_3Ph	6-Br	515	2.71	−51.3	−49.6
16[c]	CH_3	*p*-OCH_3Ph	H	622	2.79	−47.0	−46.1
17	CH_3	*m*-CH_3Ph	H	606	2.78	−48.1	−48.7
18	CH_3	*p*-CH_3Ph	H	1773	3.25	−45.0	−46.6
19	CH_3	*m*-ClPh	H	1315	3.12	−45.9	−49.4
20	CH_3	*p*-CH_2CH_3Ph	H	306	2.49	−43.5	−43.3
21	CH_3	*p*-$CH_2CH_2CH_3$Ph	H	1134	3.05	−40.4	−44.7
22	CH_3	*o*,*m*-$(CH_3)_2$Ph	H	373	2.57	−49.5	−47.4
23	CH_3	*m*,*p*-$(CH_3)_2$Ph	H	140	2.15	−47.2	−48.8
24	CH_3	1-naphthyl	6-CH_3	11	1.04	−54.8	−54.7
25	CH_3	1-naphthyl	7-OCH_3	10	1.00	−56.3	−56.4
26	CH_3	1-naphthyl	6-Br	10	1.00	−55.8	−55.7
27[d]	CH_3	1-naphthyl	H	37	1.57	−51.0	−51.2
28	H	1-naphthyl	6-CH_3	3.5	0.54	−55.4	−54.0
29	H	1-naphthyl	5-F	35	1.54	−51.7	−52.1
30	H	1-naphthyl	5-Br	186	2.27	−50.1	−54.0
31	H	1-naphthyl	5-OH	70	1.85	−54.3	−53.9
32	Cl	1-naphthyl	H	10	1.00	−52.9	−51.6
33	H	1-(4-CH_3)naphthyl	H	2.8	0.45	−55.0	−52.4
34	CH_3	1-(4-CH_3)naphthyl	H	5.9	0.77	−53.5	−53.4
35	H	1-(4-CH_3O)naphthyl	H	1.4	0.15	−56.4	−52.8
36	CH_3	1-(4-CH_3O)naphthyl	H	55	1.74	−54.3	−53.7
37	H	1-(4-OH)naphthyl	H	3.4	0.53	−56.1	−53.1
38	CH_3	1-(4-CN)naphthyl	H	15	1.18	−53.7	−53.5
39	CH_3	1-(4-Br)naphthyl	H	6.9	0.84	−54.0	−53.9
40	H	4-benzofuryl	H	24	1.38	−48.2	−49.1
41	H	7-benzofuryl	H	71	1.85	−47.6	−50.1

[a] From heterologous displacement of [^{3}H]WIN55212-2. [b] Abbreviations: *p*-OCH_3Ph, p-methoxyphenyl; 1-(4-CH_3)naphthyl, 1-(4-methyl)naphthyl; 1,2,3,4-H_4-naphthyl, 1,2,3,4-tetrahydro-1-naphthyl; etc. [c] 2-(4-Thiomorpholinyl)ethyl instead of 2-(4-morpholinyl)ethyl. [d] 2-(1-Piperidinyl)ethyl instead of 2-(4-morpholinyl)ethyl.

hydrophobic pocket of the binding site for cannabinoid agonists was also important for AAI agonist binding. Molecular docking simulations were performed to identify possible binding conformations of **1** by constraining the TM backbone of the CB_1 receptor as it would appear in the ground-state homologous to the inactive rhodopsin X-ray structure.[34] These binding conformations of **1** were grouped into two categories: in the *aroyl-down* conformations, the naphthyl ring occupies the P1 hydrophobic pocket and is positioned downward away from the extracellular side; in the *aroyl-up* conformations, the naphthyl ring occupies either of the remaining two pockets close to the extracellular side (Figure 3B,C). From the present study, by correlating the calculated binding energy (ΔE_{bind}) values versus the experimentally measured binding affinity data for a series of 37 AAI analogues (Table 1), the two best binding conformations, *aroyl-up1* ($R^2 = 0.64$) and *aroyl-up2* ($R^2 = 0.52$) (Figures 3 and 4), were assigned as the putative binding conformations for **1** at the AAI binding sites of the CB_1 receptor. The best *aroyl-down* conformation was not considered further due to the relatively poor correlation ($R^2 = 0.37$).

The present binding energy analysis showed that the CB_1 receptor−**1** interactions were predominantly van der Waals rather than Coulombic in nature (Table 2) and that distinct aromatic residues were involved in aromatic−aromatic interactions with the ligand **1** (Table 3) showing the equilibrium intermolecular distances between the aromatic rings around 4−7 Å with the reported T-shaped (T), slipped-parallel (SP), and parallel (P) geometries.[40−42]

According to the *aroyl-up1* binding conformation of **1**, the key binding site residues within 3 Å of the bound ligand

Table 2. Nonbonding Interaction Energies between **1** and the Key CB_1 Receptor Binding Site Residues within 3 Å of the Ligand

		nonbonding interaction energy (kcal/mol)		
1	CB_1 receptor	Coulombic	van der Waals	total
		(a) *Aroyl-up1*		
indole[a]	L3.29(193)	−0.03	−2.20	−2.23
	E(258)[b]	0.09	−1.20	−1.11
	K(259)[b]	−0.05	−0.83	−0.88
	Q(261)[b]	−0.12	−2.95	−3.07
	F7.35(379)	−0.40	−3.72	−3.76
	S7.39(383)	−0.06	−2.95	−3.01
naphthyl	F2.61(174)	−0.03	−3.18	−3.21
	K3.28(192)	−0.29	−2.31	−2.60
	M7.40(384)	0.03	−2.02	−1.99
	L7.43(387)	0.03	−0.99	−0.96
morpholinyl	V3.32(196)	0.04	−2.34	−2.30
	T3.33(197)	0.04	−0.95	−0.92
	L6.51(359)	0.03	−1.78	−1.75
	C7.42(386)	0.07	−0.97	−0.90
		(b) *Aroyl-up2*		
indole[a]	L3.29(193)	0.00	−2.25	−2.25
	N(256)[b]	−0.09	−1.45	−1.54
	C(257)[b]	0.18	−1.46	−1.28
	E(258)[b]	0.01	−1.66	−1.65
	Y5.39(275)[c]	−0.10	−4.60	−4.70
naphthyl	K(259)[b]	−0.27	−3.15	−3.42
	L(260)[b]	0.03	−1.68	−1.65
	I5.35(271)	0.01	−0.81	−0.80
	M7.40(384)	0.04	−0.46	−0.42
	D7.22(366)	−0.32	−1.53	−1.85
	K7.26(370)	0.08	−1.09	−1.01
	K7.29(373)	0.17	−0.55	−0.38
morpholinyl	V3.32(196)	−0.01	−0.61	−0.62
	T3.33(197)	−0.20	−2.49	−2.69
	F3.36(200)	0.05	−1.40	−1.35
	I4.56(247)	0.02	−0.78	−0.76
	F5.42(278)	0.01	−1.51	−1.50
	W6.48(356)	0.01	−0.70	−0.69
	M6.55(363)	0.05	−1.96	−1.91

[a] To each moiety of the ligand, the receptor residues were assigned by visual inspection. [b] Residues in E2. [c] Also important for the naphthyl ring (see Table 3).

1 were as follows (Table 2 and Figure 5A(i)): for the indole ring, L3.29(193), E(258), Q(261), F7.35(379), and S7.39(383); for the naphthyl ring, F2.61(174), K3.28(192), M7.40(384), and L7.43(387); and for the morpholinyl moiety, V3.32(196) and L6.51(359). No H-bonding interaction was observed in the *aroyl-up1* binding conformation. The aromatic−aromatic interaction between F2.61(174) with the naphthyl ring, and F7.35(379) with the indole ring appeared to be important for the receptor−ligand interaction (Figure 5B(i) and Tables 2 and 3). F2.61(174) was also involved in aromatic−aromatic interactions with H2.65(178) and F2.64(177) that interacted in turn with F3.25(189) (Table 3 and Figure 5B(i)). Thus, the *aroyl-up1* conformation formed an aromatic cluster using residues in TMs 2−3, which were quite different from those residues in TMs 3−5 reported by Song et al.[20] There have been no mutational studies on these aromatic residues for the CB_1 receptor; it was reported, however, that the mutation of D2.50(163) of the CB_1 receptor to Glu or Asn resulted in a significant reduction of binding for **1** but not for other classes of the CB_1 ligand.[43] Nevertheless, recent studies of the dopamine D_2 and D_4 receptors[44] and CCR5[45] suggested possible involvement of cluster-forming aromatic residues between TMs 2−3 in ligand binding and receptor activation.

According to the *aroyl-up2* binding conformation of **1**, the key binding site residues within 3 Å of the bound ligand **1** were as follows (Table 2 and Figure 5A(ii)): for the indole ring, L3.29(193), N(256), C(257), E(258), and Y5.39(275); for the naphthyl ring, K(259), L(260), D7.22(366), and K7.26(370); and for the morpholinyl moiety, T3.33(197), F3.36(200), F5.42(278), and M6.55(363). About half of the binding site residues in the *aroyl-up2* conformation are from the TM4-E2-TM5 region, which has been suggested to be critical for **1** binding from a chimeric CB_1/CB_2 receptor study.[46] Two H-bonding interactions were observed in this binding conformation: the one between the amide NH of K(259) and the C3 carbonyl oxygen of the ligand and the other between the side chain OH of T3.33(197) and the fused ring oxygen. The latter would not be possible for any of the compounds listed in Table 1, and therefore the binding energies and the IC_{50} values for these compounds would not have been influenced by this potential H-bonding interaction. For the *aroyl-up2* conformation, the aromatic−aromatic interaction between Y5.39(275) with both the naphthyl ring and the indole ring appeared to be important for the receptor−ligand binding (Tables 2 and 3). It was shown that

Table 3. Key Aromatic Clustering and Binding Interactions for **1**: (a) in the *Aroyl-up1* Conformation and (b) in the *Aroyl-up2* Conformation

		distance[a]	plane angle[b]	geometry[c]
		(a) *Aroyl-up1*		
F2.61(174)	naphthyl (first phenyl)	3.8	25	P
F2.61(174)	naphthyl (second phenyl)	4.3	25	P
F7.35(379)	indole (phenyl)	5.4	86	T
F7.35(379)	indole (pyrrole)	5.2	86	T
F2.61(174)	F2.64(177)	4.5	40	SP
F2.61(174)	H2.65(178)	4.8	77	T
F2.64(177)	H2.65(178)	4.8	45	SP
F2.64(177)	F3.25(189)	6.4	72	T[d]
		(b) *Aroyl-up2*		
Y5.39(275)	naphthyl (first phenyl)	5.9	76	T
Y5.39(275)	naphthyl (second phenyl)	5.3	76	T
Y5.39(275)	indole (phenyl)	7.1	41	SP
Y5.39(275)	indole (pyrrole)	5.7	41	SP
F3.36(200)	W6.48(356)	5.8	25	P
Y5.39(275)	F5.42(278)	7.2	86	T
F5.42(278)	W6.48(356)	7.4	69	T

[a] The distance between the centroids, in Å. [b] The angle between the ring planes, in degrees. [c] P: parallel; SP: slipped-parallel; and T: T-shaped (refs 40−42). [d] Not exactly edge-to-faced.

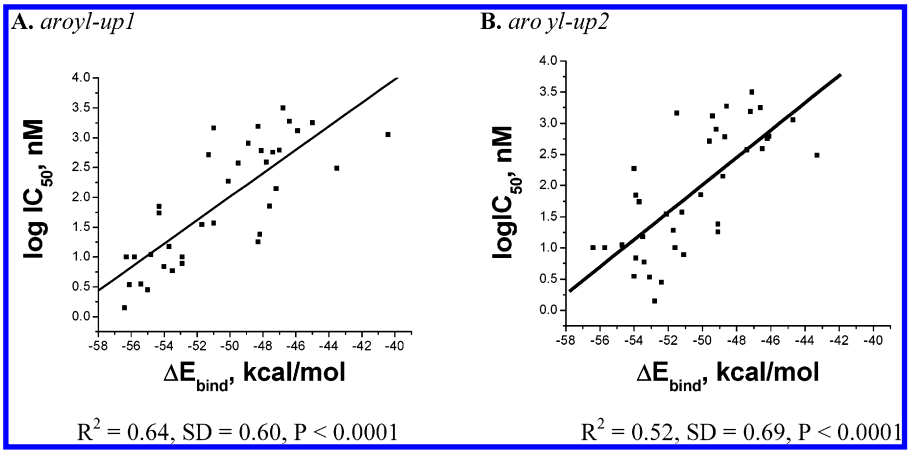

Figure 4. Correlation between experimental CB_1 receptor affinity for the [^{3}H]WIN55212-2 binding site (log IC_{50}, IC_{50} in nM)[16] versus calculated binding energy (ΔE_{bind} in kcal/mol) for 37 AAI analogs, using the *aroyl-up1* (A) and *aroyl-up2* (B) conformations. The approximation was made that $\Delta E_{bind} \cong \Delta G_{bind} \propto \log IC_{50}$. Linear regression parameters: R^2, the square of R, the correlation coefficient; SD, standard deviation of the fit; and P, probability that R is zero.

Y5.39(275) was also involved in aromatic−aromatic interactions with F5.42(278) and W6.48(356) (Table 3 and Figure 5B(ii)). In agreement, it has been proposed that the CB_1 Y5.39(275) is important for aromatic interaction with the ligand.[46,47] Our *aroyl-up2* conformation formed an aromatic cluster using the residues quite similar to those in the model of Song and colleagues.[20]

Rotational Energy Barrier Calculations of 1. To elucidate how the ligand can induce receptor conformational change, we have adapted the steric trigger mechanism proposed originally for the covalently bound retinal within rhodopsin[48] to the diffusible cannabinoid ligands within the CB_1 receptor.[30] In our previous study, we proposed that the released strain energy from the bound ligand **2** to the receptor would be the driving force for inducing receptor conformational changes necessary for transferring signal to G-proteins. We demonstrated that the ligand strain energy could be released by rotating the first two torsion angles of the C3 side chain (i.e., as the steric trigger) to allow **2** to attain the lowest possible energy conformation, creating an unfavorable steric clash with the receptor hydrophobic pocket. The ACD-ring moiety, interacting with residues in the P2 pocket, served as the plug to provide a stable ligand-receptor association.[30] Release of the energy of the constrained ligand, imposed by the binding to the ground state of the receptor (R), would allow for adjustments along the receptor helices that could initiate activation of the receptor (R*) and its associated G-protein.[30] Thus, to be qualified as the steric trigger, the moiety first of all should be conformationally flexible (i.e., energetically easy to rotate). In the present study, to characterize the conformational flexibility properties of **1**, rotational energy barriers were estimated by torsional driver calculations, using MMFF94, AM1, and *ab initio* HF/3-21G(*) methods. Four rotatable torsion angles in **1** were defined as follows: τ1(C2═C3−C═O), τ2(C3−C(═O)−C1′−C2′), τ3(N1−C10−C11−N12), and τ4(C10−C11−N12−C13) (Figure 1). All three calculation methods showed similar energy profiles (Figure 6A). Rotation around τ1 showed high rotational energy barriers at around 90° and −90° (5−10 kcal/mol), where the C═O bond becomes perpendicular to the C2═C3 bond. Rotation around τ2 showed two rotational energy barriers at around 0° (<5 kcal/mol) and at around 180° (∼10 kcal/mol), where the aroyl moiety becomes eclipsed to the indole ring moiety to cause sterically unfavorable interactions. Rotations around τ3 and τ4 showed rather more complex energy profiles due to the presence of the heterocyclic systems comprised of the morpholine and indole rings. These calculations revealed that all the ligand moieties would be rotatable without high-energy barriers, suggesting that **1** could be freely induced to best-fit to the receptor pocket by adjusting any of these torsion angles of the ligand. Thus, it is possible that multiple **1**−CB_1 receptor binding conformations may exist depending upon the receptor state.[49]

MD Simulations of 1. To examine the tendency of **1** to change its conformation after being bound to the ground state of the CB_1 receptor, MD simulations in the absence of the receptor were performed. All four rotatable torsion angles, τ1−τ4, were analyzed by 35 ns MD simulations at 300 K for both the *aroyl-up1* (Figure 7) and *aroyl-up2* (Figure 8) conformations, starting from the initial ground-state receptor-bound ligand conformation, defined as **STATE_i1** and **STATE_i2**, respectively. The MD simulations showed fluctuation in structure and energy. The most striking change was noticed in τ1 and its associated energy (Figures 7 and 8): The ligand existed as *s-trans* in its initial receptor-bound states, **STATE_i1** and **STATE_i2**. These conformations were 3−5 kcal/mol higher in energy than the *s-cis* states in the relaxed conformation, defined as **STATE_f1** and **STATE_f2**. The change in the torsion angle value of τ2 seemed to be associated with the torsion angle value of τ1. As shown in Figure 9A, conversion of τ1 from *s-trans* to *s-cis* can occur by adjusting the torsion angle of τ2 to reduce the steric repulsion to the indole ring in order to traverse the lowest possible rotational energy barrier within the allowed conformational space. This is well illustrated in the case of the *aroyl-up1* conformation, for which the aroyl ring was flipped to change τ2 from 79° to −69°. In contrast, for the *aroyl-up2* conformation, the aroyl ring did not adjust, possibly due to the insignificant steric repulsion between the aroyl and indole rings during τ1 change. Consistently, it was revealed that the major contributions to the energy difference in the *s-trans* to *s-cis* transition could be attributed to bend, torsion, and van der Waals (Table 4).

As shown in Figures 7(i) and 9, structural transition for the *aroyl-up1* conformation occurred at τ1 = −74.8° and

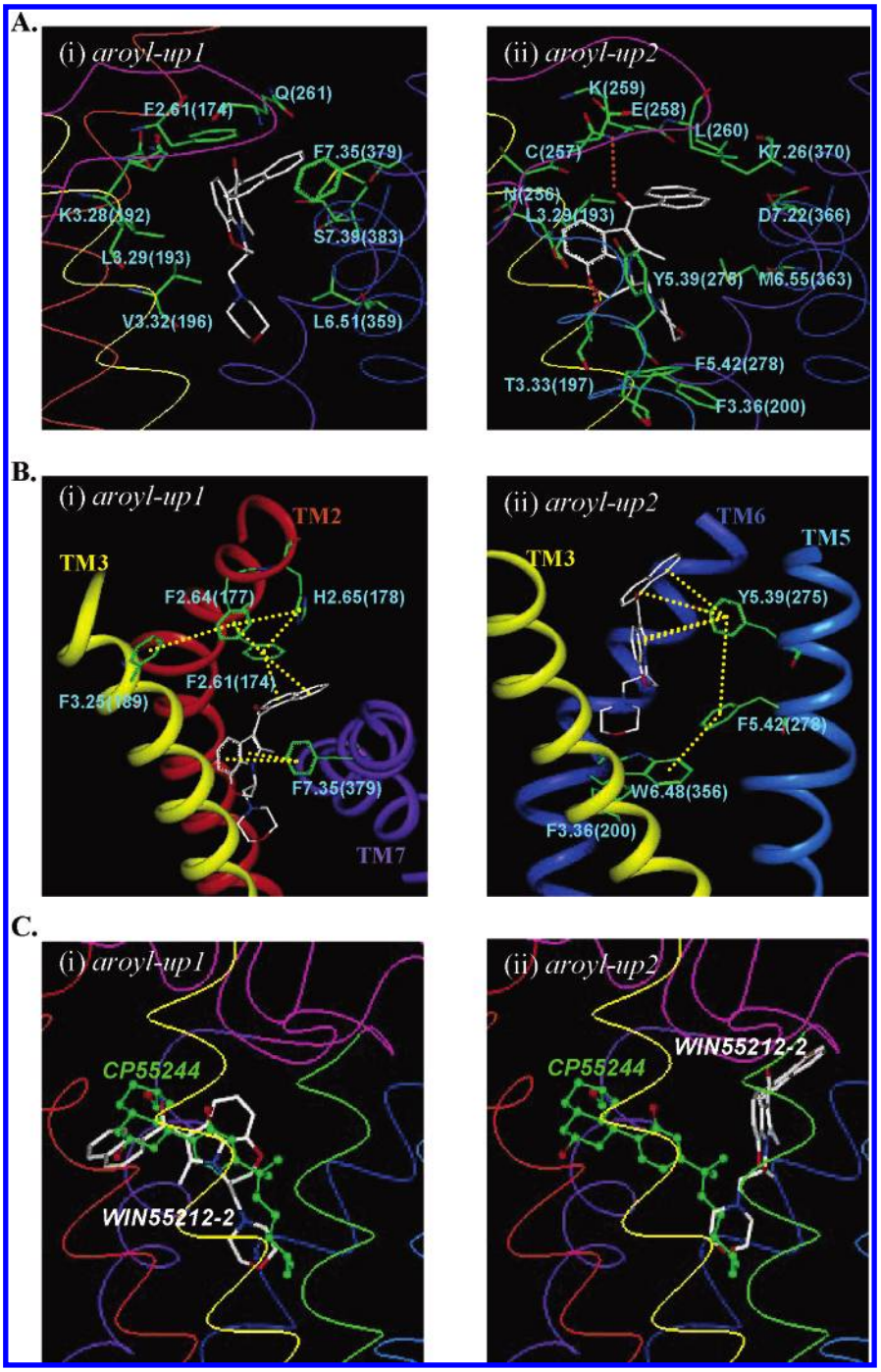

Figure 5. Binding conformations of **1** in the CB_1 receptor. Color coding of ligand atoms: white, C; red, O; and blue, N. Color coding of receptor residue atoms: green, C; red, O; and blue, N. Parts of TM2−TM7 are colored in orange, yellow, green, cyan, blue, and purple, respectively. The extracellular loops are colored in magenta. A. Key binding interactions of **1** with amino acid residues of the CB_1 receptor for (i) *aroyl-up1* and for (ii) *aroyl-up2*. H-bonding is indicated in dotted lines (in orange). B. Key aromatic−aromatic interactions (in dotted lines) between **1** ((i) *aroyl-up1* and (ii) *aroyl-up2*) and the pocket residues (see text). C. Receptor-derived superimposition models for **1** and **2**. The binding conformations of **1** ((i) *aroyl-up1* and (ii) *aroyl-up2* in stick depiction) and **2** (in green ball-and-stick depiction) were RMSD fitted using the receptor TM backbone structures.

$\tau 2 = 0.1°$ in 5.12 ns, traversing an energy barrier of ~8 kcal/mol. Similarly, as shown in Figures 8(i) and 9, structural transition for the *aroyl-up2* conformation occurred at $\tau 1 = -75.2°$ and $\tau 2 = 75.6°$ in 4.93 ns, traversing an energy barrier of ~10 kcal/mol. After this state, the ligand remained in a conformation low in energy due to the release from the ligand strain energy. Throughout the entire MD simulations, the values of $\tau 3$ and $\tau 4$ remained unchanged around 180° and −70°, respectively (Figures 7 and 8, and Table 4) with the values quite similar for the initial, receptor-bound conformation, indicating that the morpholinyl moiety would not play a role in a receptor conformational change.

DISCUSSION

Comparison of the Binding Conformations of 1 and 2. To understand the similar cannabimimetic activity of the structurally diverse cannabinoids and AAIs, some efforts have been made to derive ligand-based superimposition models of cannabinoids and AAIs by fitting pharmacophoric atoms of the ligands.[16,50−52] Huffman et al.[50] superimposed

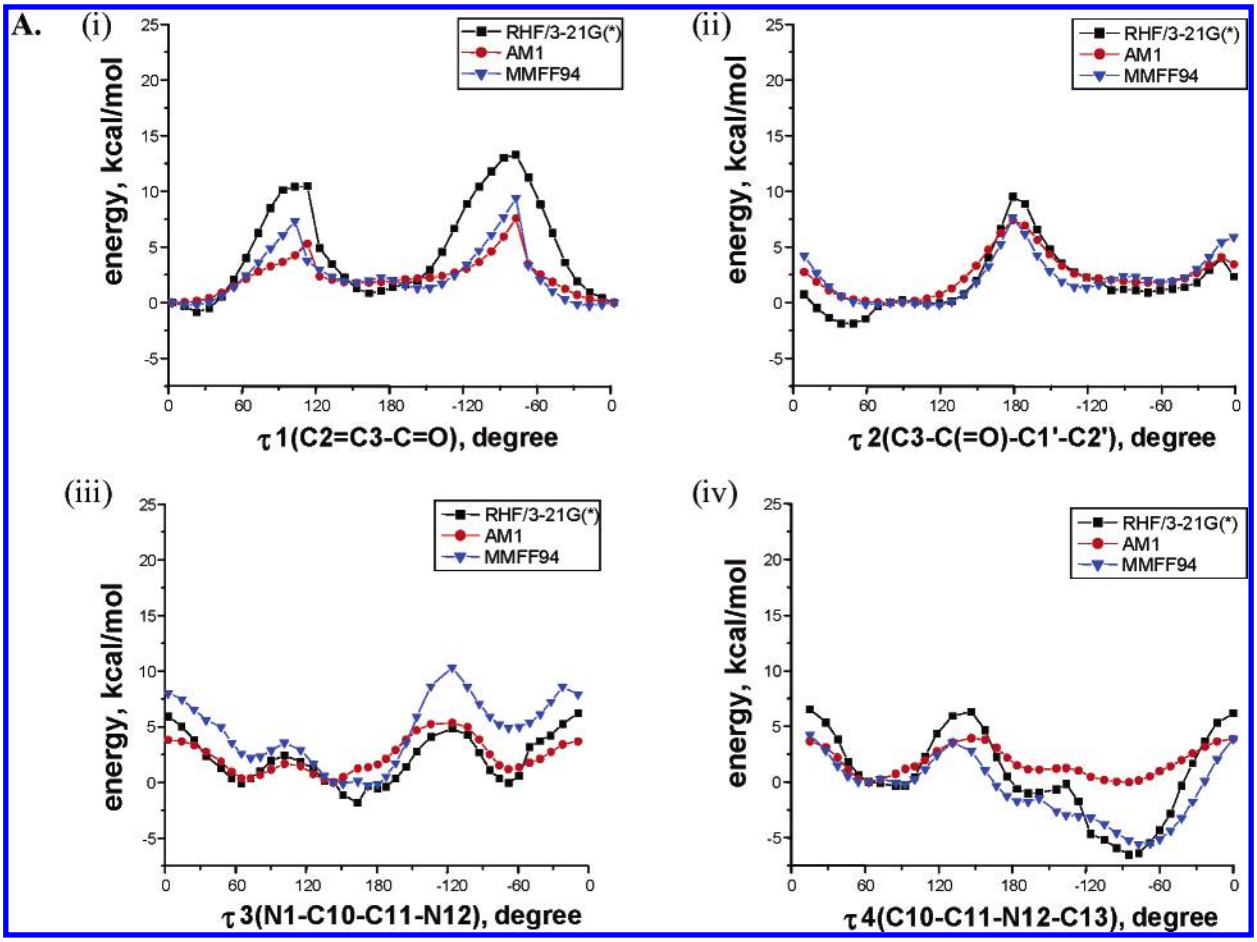

Figure 6. A. MMFF94, AM1, and HF/3-21G(*)-derived rotational energy barriers (in kcal/mol) of **1** calculated for (i) τ1, (ii) τ2, (iii) τ3, and (iv) τ4.

the C3 side chain of the cannabinoids and the aminoalkyl moiety of the AAIs. In contrast, Xie et al.[51] and Shim et al.[52] superimposed the C3 side chain of cannabinoids and the aroyl group of the AAI. Whereas a ligand-based superimposition model is solely based upon probable conformations of the receptor-free ligands, a receptor-based superimposition would provide a more realistic model with the ligand conformations in the receptor environment. The present receptor-based superposition models of **1** and **2** were derived by root-mean square deviation (RMSD) fitting of the receptor TM backbone structures of the binding conformations of **1** (*aroyl-up1* and *aroyl-up2*) to that of **2**.[12] These models agreed with the ligand-based model by Huffman et al.[50] with respect to alignment of the aminoalkyl moiety of AAIs to the C3 side chain of cannabinoids in pocket P1 (Figure 5C). In support of Huffman's ligand-based model,[50] a pentacyclic derivative developed by Huffman et al.,[53] hybridizing the classical cannabinoids and AAIs, showed similar binding affinity and in vivo activity to Δ^8-THC. Compared with this pentacyclic derivative where the cannabinoid A-ring was introduced next to the indole ring of the AAIs, our superposition model from *aroyl-up1* suggested a potentially better hybrid cannabinoid by positioning the cannabinoid A-ring to the pyrrole ring portion of the AAIs. It appears that this position occupied by aromatic residues of both classes of cannabinoids would be important for ligand binding.

Based on the present superimposition model of **1** in *aroyl-up1* and **2** (Figure 5C(i)), common pharmacophoric elements would be as follows: (1) the indole ring moiety of **1** and the A-ring moiety of **2**; (2) the morpholinyl moiety of **1** and the C3 side chain of **2**; and (3) the aroyl group of **1** and the C/D-ring moiety of **2**. In contrast, the superposition model of **1** in *aroyl-up2* and **2** (Figure 5C(ii)) shares only one common pharmacophoric element, the morpholinyl moiety of **1** and the C3 side chain of **2**. Evidence from competitive binding assays[16−19] supports such models in which these two structurally different classes of CB_1 receptor agonists can compete for common binding site residues, such as the hydrophobic P1 pocket. Binding energy analyses suggested that hydrophobic interactions by the P1 pocket residues in TMs 3−6 were the most important for **2**, while aromatic−aromatic interactions by the receptor pocket aromatic residues were the most important for **1**.

Is the C3 Carbonyl Oxygen of AAI Agonists Critical for Receptor Interaction? It was observed that AAI structural analogues devoid of the carbonyl oxygen of the aroyl moiety showed an increased binding affinity compared with the corresponding AAI compound.[17,54,55] This finding would suggest that the C3 carbonyl oxygen and its possible H-bonding would not be important for AAI binding to the CB_1 receptor. In the present study, the C3 carbonyl oxygen of **1** formed no H-bond in the *aroyl-up1* binding conformation, while it formed one H-bond with the backbone nitrogen of K(259) in the *aroyl-up2* binding conformation. It appears, however, that K(259) in *aroyl-up2* would contribute to ligand binding through hydrophobic interaction (with the naphthyl moiety) rather than through H-bonding (with the C3 carbonyl oxygen) (Table 2). Chin et al.[56] proposed that an increase in

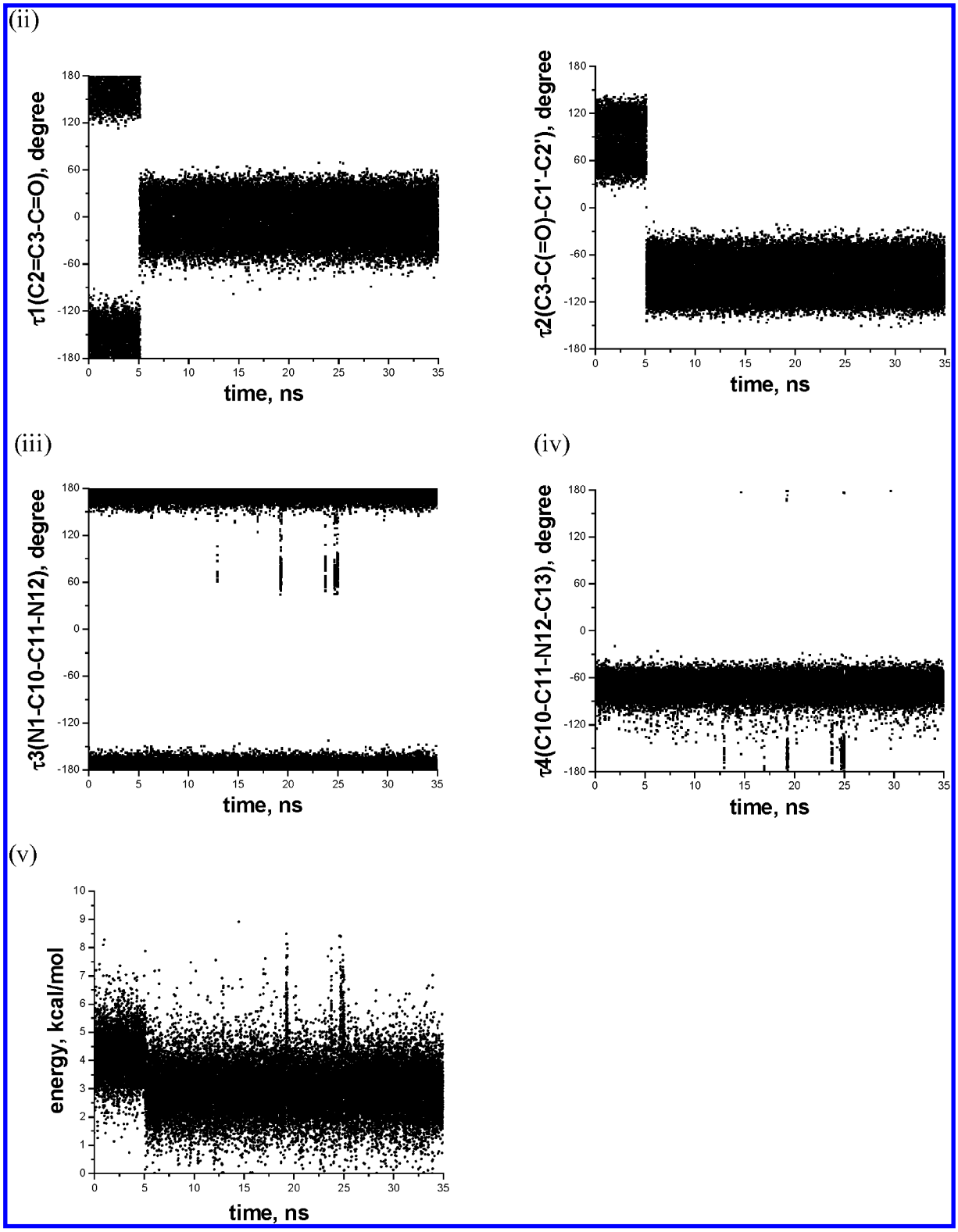

Figure 7. Conformational preference of **1** in *aroyl-up1*, starting from **STATE_i1**, calculated for the individual torsion angles, (i) τ1, (ii) τ2, (iii) τ3, and (iv) τ4, along with (v) the ligand internal energy during a 35 ns MD simulation at 300 K.

binding affinity for AAIs by G3.31(195)S mutation in the CB_1 receptor would be due to the formation of an H-bond with the C3 carbonyl oxygen of AAIs. From our CB_1 receptor model, G3.31(195) is facing a region of TM3 opposite to the binding pocket-forming residues, L3.29(193), V3.32(196), and T3.33(197), suggesting that it is not probable that a residue in the position of G3.31(195) is involved in any direct binding interaction with **1**. Thus, any increased binding to the CB_1 receptor by the G3.31(195)S mutation could be attributed to a modification of the receptor helical orientation rather than a direct interaction with the ligand. Together with the known SAR for the indene class of AAI analogues,[17,54,55] showing the retained binding affinity despite the absence of the C3 carbonyl oxygen, our models suggested that the C3 carbonyl oxygen of AAI agonists would not be critical for receptor interaction.

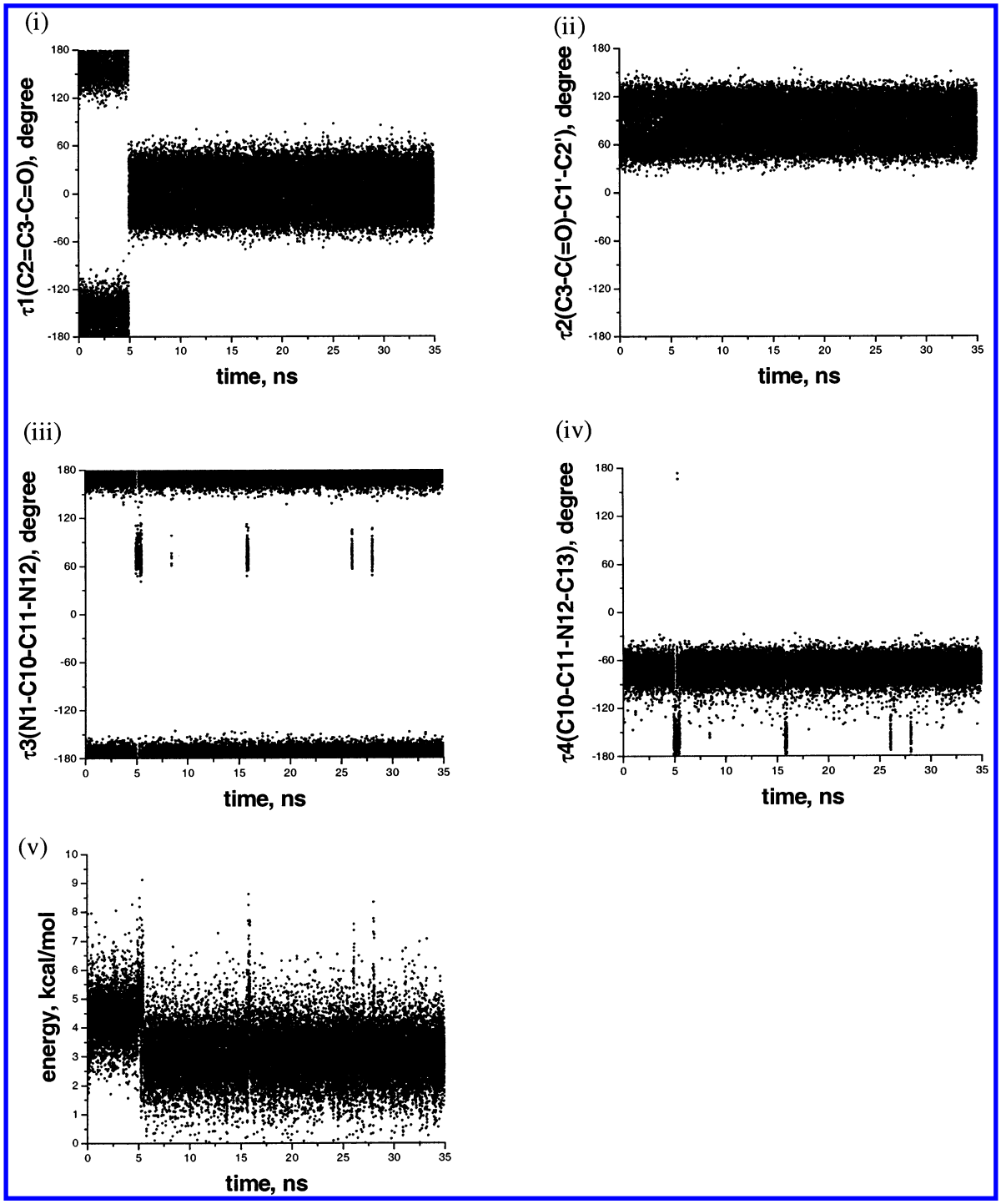

Figure 8. Conformational preference of **1** in *aroyl-up2*, starting from **STATE_i2**, calculated for the individual torsion angles, (i) τ1, (ii) τ2, (iii) τ3, and (iv) τ4, along with (v) the ligand internal energy during a 35 ns MD simulation at 300 K.

Steric Trigger Mechanism for 1-Induced Receptor Conformational Change. In the case of rhodopsin, it is known that the high energy of photoisomerization (~35 kcal/mol)[57,58] is necessary to rapidly induce the activation process.[59] This corresponds to the energy barrier for the rotation around the C11═C12 bond of the covalently bound retinal. However, in the case of aminergic GPCRs with diffusible ligands, receptor activation appears to occur over a slower time course with much smaller energy.[59] For example, the energy available for conformational change in the β_2 adrenergic receptor was estimated to be only 6−10 kcal/mol upon the basis of its ligand binding energy.[59] The difference in activation energy and rate between these two receptor activation mechanisms might reflect different pathways of microconformational changes that must occur to achieve an activated state.[49,60,61]

As demonstrated in our present MD simulations, the ligand strain energy of **1** as found in the receptor-bound form was released by changing the τ1 torsion angle from *s-trans* to *s-cis*. It was calculated that the ground-state receptor bound conformations of **1** (**STATE_i1** and **STATE_i2**) were about 3−5 kcal/mol higher in energy than those of the lowest energy *s-cis* conformations identified by both the systematic and MC search methods (Table 4). We propose that this

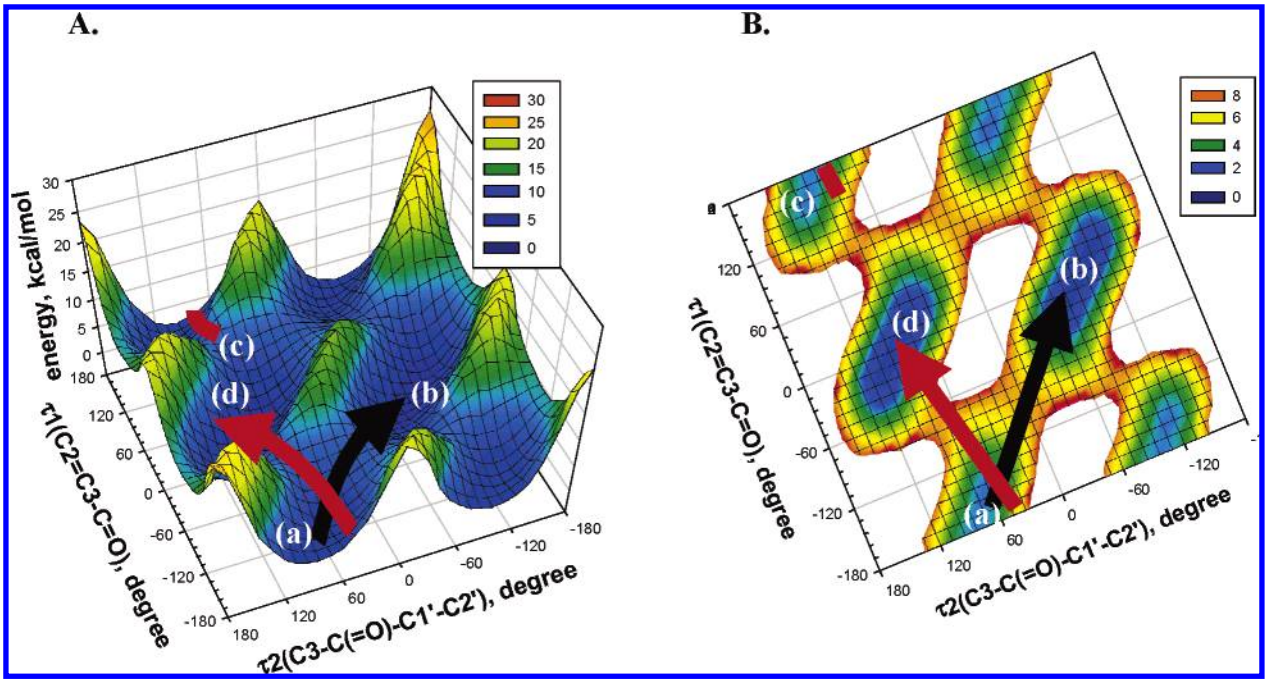

Figure 9. A. 3D mesh plot of rotational energy barriers (in kcal/mol) of **1** calculated for a combination of $\tau 1$ and $\tau 2$. The torsional drivers for $\tau 1$ and $\tau 2$ were taken in 10° increments for the range of 360°. The plot was created using a local smoothing technique that computes the median of the energy values at neighboring points. B. Energy contour plot of rotational energy barriers (in kcal/mol) of **1** calculated for a combination of $\tau 1$ and $\tau 2$. Contours are drawn at 2 kcal/mol increments above the lowest energy conformation found. Paths were depicted by the arrow that takes the lowest energy path suggested from the conformational analyses, starting from **STATE_i1** (a) and progressing to **STATE_f1** (b) for the *aroyl-up1* (in black) and from **STATE_i2** (c) and to **STATE_f2** (d) for the *aroyl-up2* (in red).

Table 4. Comparison of the Lowest Energy Conformations Determined from the Conformational Analysis (see the Computational Methods Section) with the Ground-State Receptor-Bound Conformations **STATE_i1** and **STATE_i2** of **1** Determined from the Present Docking Study and **STATE_f1** and **STATE_f2** of **1** Generated from the 35 ns MD Simulations

	systematic search	MC search	STATE_i1[a]	STATE_i2[a]	STATE_f1[b]	STATE_f2[b]
			Torsion Angles, degree			
$\tau 1$(C2═C3−C═O)	16 (*s-cis*)	−18 (*s-cis*)	−172 (*s-trans*)	155 (*s-trans*)	−20 (*s-cis*)	18 (*s-cis*)
$\tau 2$(C3−C(═O)−C1′−C2′)	−110	110	79	87	−69	69
$\tau 3$(N1−C10−C11−N12)	180	180	174	180	180	180
$\tau 4$(C10−C11−N12−C13)	−69	−69	−76	−69	−69	−69
			Energy Components, kcal/mol			
stretch	8.79	8.80	8.26	8.66	8.73	8.72
bend	13.22	13.15	13.27	14.58	12.84	12.94
torsion	2.06	2.14	3.82	4.33	2.21	2.10
stretch−bend	0.50	0.50	0.49	0.55	0.50	0.50
out-of-plane	0.02	0.02	0.05	0.09	0.04	0.04
1−4 van der Waals	70.44	70.46	71.19	70.25	70.63	70.60
other van der Waals	−2.25	−2.34	−1.04	−1.27	−2.17	−2.12
1−4 electrostatic	4.03	4.02	3.33	3.34	3.91	3.91
other electrostatic	2.78	2.79	3.43	3.53	2.89	2.88
E_{total}	99.58	99.54	102.79	104.04	99.58	99.58

[a] To obtain the ground-state receptor-bound conformations **STATE_i1** and **STATE_i2**, the CB_1 receptor−**1** docking complex generated using the CFF force field was subjected to full energy minimization using the MMFF94 force field. Only receptor residues within 6 Å of **1** were included while other residues were held fixed. Then, **1** was extracted and subjected to a single point energy calculation. [b] Fully energy minimized structure after average over the last 5000 trajectories, using the MMFF94 force field.

released ligand strain energy could provide a driving force for a receptor microconformational change that could initiate the activation mechanism.

We propose that the aroyl moiety of AAI agonists would serve as the steric trigger, just like the C3 side chain of **2** for receptor activation.[30] The aroyl moiety as the steric trigger would be a reasonable choice, because this moiety appeared to cause a steric clash with aromatic residue(s) that forms aromatic clusters, thereby effectively promoting the disruption of interhelical interactions. Based upon our present binding conformations of **1**, it appears that F2.61(174) in *aroyl-up1* and Y5.39(275) in *aroyl-up2* would be important targets for destabilizing the ground-state aromatic−aromatic interactions (Table 3 and Figure 5).

The steric trigger mechanism requires a plug point to fix a portion of the ligand in the receptor binding space to efficiently trigger a receptor conformational change. In the case of **2**, the ACD ring, including a critical H-bond between the A-ring OH and the K3.28(192), could serve as the plug for ligand−receptor association.[30] It appears that the indole

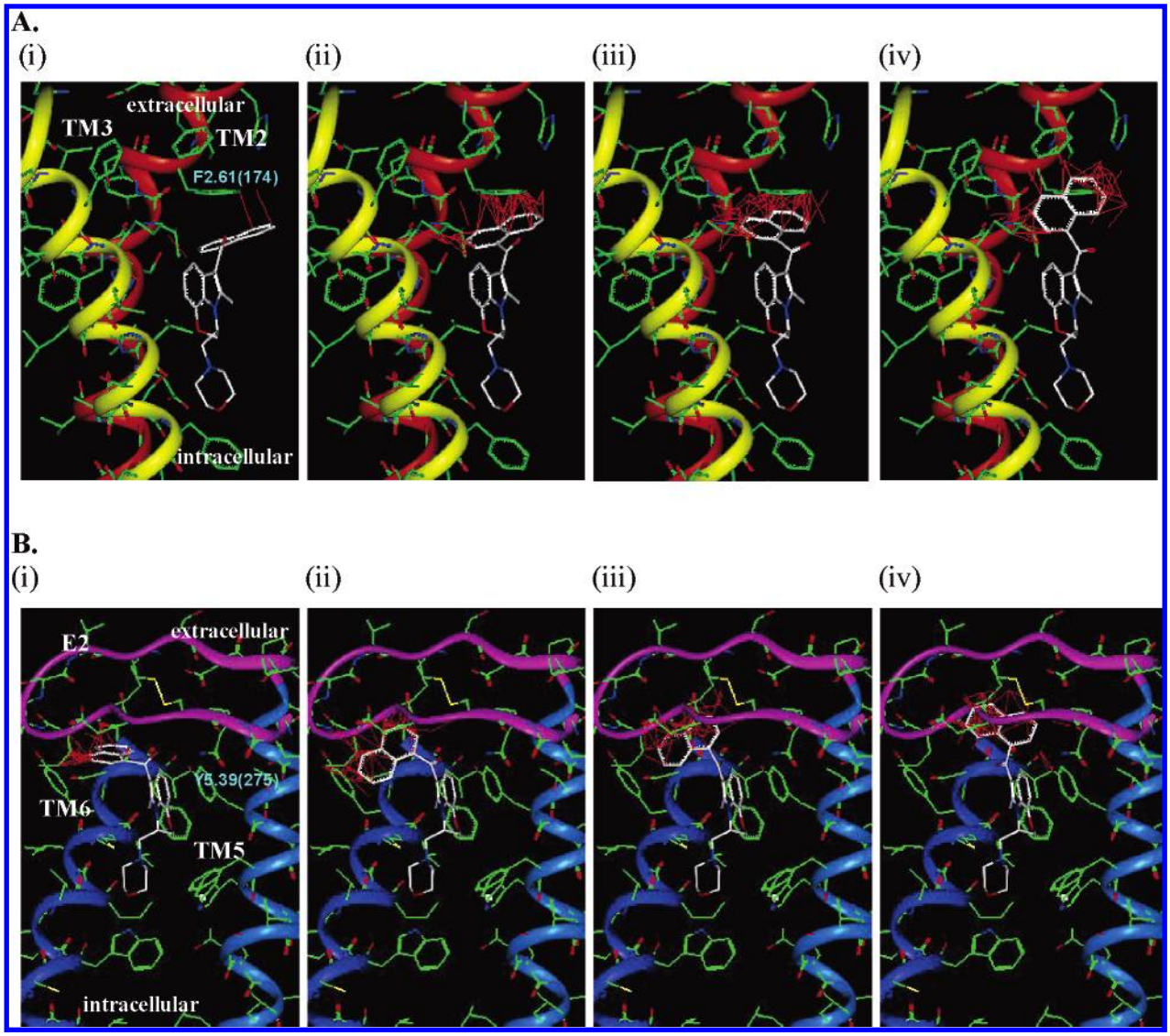

Figure 10. Possible steric clash by the rotation of the aroyl moiety in the *aroyl-up1* and *aroyl-up2* binding conformations. The naphthyl ring of **1** (in stick depiction) functions as the steric trigger for inducing a receptor conformational change (see text). For the rotation of the aroyl moiety, the paths demonstrated by the conformational analyses in Figure 9 were used. A. *Aroyl-up 1*: Depiction of the rotation of the naphthyl moiety starting from $\tau1 = -172°$, $\tau2 = 79°$ (**STATE_i1**): (i) $\tau1 = -141°$, $\tau2 = 55°$; (ii) $\tau1 = -112°$, $\tau2 = 42°$; (iii) $\tau1 = -84°$, $\tau2 = 48°$; and (iv) $\tau1 = -20°$, $\tau2 = -69°$ (**STATE_f1**). Probable steric clash with TM2 and TM3 is shown as red lines connecting the naphthyl ring structure with the receptor moieties that obstruct free rotation. B. *Aroyl-up 2*: Depiction of the rotation of the naphthyl moiety starting from $\tau1 = 155°$, $\tau2 = 87°$ **STATE_i2**): (i) $\tau1 = -113°$, $\tau2 = 50°$; (ii) $\tau1 = -66°$, $\tau2 = 125°$; (iii) $\tau1 = -30°$, $\tau2 = 118°$; and (iv) $\tau1 = 18°$, $\tau2 = 69°$ (**STATE_f2**). Probable steric clash with E2 and TM5 is shown as red lines connecting the naphthyl ring structure with the receptor moieties that obstruct free rotation. TM2, TM3, TM5, and TM6 backbones are colored in orange, yellow, cyan, and blue, respectively. Color coding of receptor atoms: green, C; red, O; and blue, N. Color coding of **1** atoms: white, C; red, O; and blue, N.

ring moiety of **1** may perform a similar role as the plug, as indicated by its major contribution to receptor binding association (Table 2). It also appears that the morpholine moiety of **1** is fairly constrained due to the ring connecting positions 7 and 10, making it likely to contribute to the plug function based on our MD simulation showing that the value of $\tau3$ and $\tau4$ remained unchanged. However, the aminoalkyl moiety (i.e., the morpholine ring) in the AAI analogues shown in Table 1 that do not possess this ring structure may exhibit greater flexibility as the result of the introduction of an additional rotatable torsion angle $\angle$(C2−N1−C10−C11) (see Figure 1). Thus, it may be possible that the unstructured AAI analogues might exhibit different signal transduction efficacy compared with the more rigid AAIs such as **1**. For example, it was shown from the study by Kuster et al.[19] that several unstructured AAI analogues were not as efficacious as their rigid AAI counterparts for inhibiting neuronally stimulated contractions in isolated mouse vas deferens preparations despite their comparable binding affinity. Also, it was shown from the study by Huffman et al.[53] that a pentacyclic hybrid cannabinoid, which resembles **1** but with a restrained aroyl ring moiety, showed comparable affinity compared with **1** but with reduced potency for the biological responses. For this particular compound, an alternative moiety, such as the pentyl moiety, just as in Δ^9-THC, might be responsible for triggering the observed agonist activity.

Microconformational changes in the CB_1 receptor that might be induced by the receptor-bound **1** are shown in Figure 10. Starting from **STATE_i1** and proceeding to **STATE_f1** (Figure 10A), and from **STATE_i2** to **STATE_f2** (Figure 10B), the ligand conformation was modified to follow the energy path as described by the MD

simulations. Thus, the steric trigger aroyl moiety was rotated by a combination of $\tau 1$ and $\tau 2$, while the other moieties of the ligand remained in the binding pocket as the plug.

For the *aroyl-up1* conformation, rotation of the aroyl ring of **1**, as depicted in Figure 10A(i)−(iv), caused steric clash with the TM region, primarily TM2. Because the aroyl moiety interacts with F2.61(174) forming an aromatic cluster with neighboring aromatic residues [i.e., F2.64(177), H2.65(178), and F3.25(189)], the trigger effect of the aroyl ring transition could be rather significant. It would cause the disruption of the aromatic−aromatic interaction between the aroyl ring and F2.61(174) and the disruption of the aromatic cluster composed of the residues on the extracellular side of TM2 and TM3 (Table 3(a)), which would destabilize the helical interactions between TM2 and TM3. If TM2 of the CB_1 receptor is sharply bent in the middle of the helical domain, as is the case for the rhodopsin structure found in the X-ray,[34] the effect of the disruption on the extracellular side would be significant in the intracellular side. It is also possible that unfavorable steric clash with TM2 initiated by the ligand steric trigger would disrupt the proposed functional coupling between TM2 and TM7 through a potential hydrogen bonding network involving the highly conserved D2.50 and N7.49.[62]

Song and Bonner[9] reported a very slight loss of affinity for [^{3}H]WIN55212-2 when K3.28(192) was mutated to Ala. Further, Chin et al.[56] reported that the replacement of K3.28(192) by the shorter alkyl chains of Gln and Glu mutants exhibited somewhat reduced binding affinity for [^{3}H]WIN55212-2. These studies suggested that, though not critical, K3.28(192) would closely interact with **1** (Table 2). In the present *aroyl-up1* binding conformation of **1**, the naphthyl ring moiety participates in a binding interaction with K3.28(192), not via H-bonding interaction[17,54] but via hydrophobic interaction. A slight reduction in binding affinity would be expected if the hydrophobic alkyl chain were reduced to a methyl (as in Ala) or ethyl linkage before the carbonyl oxygen of the side chain terminus (as in Gln or Glu). The most important result of the K3.28(192)Q mutation was the significant loss of signal transduction in response to **1**.[56] This observation suggests a role of K3.28(192) in **1**-induced receptor activation.[10] According to the present CB_1 receptor model, E(258) directly interacts with K3.29(192) as its counterion. In the reported mutation result, E(258) would not be able to interact with the neutral Q3.28 as tightly as with the positively charged K3.28(192). Thus, the ramifications of a steric trigger mechanism involving the naphthyl group is that the TM3 interactions that stabilize the ground state of the receptor would be disrupted.

For the *aroyl-up2* conformation, rotation of the aroyl ring of **1**, as depicted in Figure 10B(i)−(iv), as the steric trigger starting from **STATE_i2** proceding to **STATE_f2** caused steric clash primarily with E2. It has been reported that, for the CB_1 receptor[46] and other aminergic GPCRs,[58] E2 is involved in ligand binding. In the present study, it appeared that the steric clash of **1** to E2 would disrupt the tight binding with Y5.39(275), leading to disruption of the aromatic cluster formed by its neighboring aromatic residues [i.e., F5.42(278), W6.48(356), and F3.36(200)], which would destabilize the ground-state receptor conformation. In agreement, it has been reported that structural destabilization of E2 resulted in constitutively active receptors.[63]

Recent studies on the β_2 adrenergic receptor by Kobilka and his colleagues demonstrated agonist-specific receptor conformational changes and functional properties.[49,60] They proposed the sequential binding model for GPCR activation to explain step-by-step binding interactions between the ligand and the receptor to form multiple receptor conformational states with distinct cellular responses.[49] In the sense that a specific ligand moiety contributes to induce a distinct receptor conformational change, the sequential binding model is analogous to our steric trigger model. However, the details of the sequential binding model as to how multiple receptor conformational states would be induced by different ligands have not been reported. In the present study, we propose that the ligand conformational change might be responsible for such states. In the same way that Kobilka and his colleagues proposed that different ligand moieties may be responsible for the interactions with different TMs,[49,60] we propose that structurally different ligands (**1** and **2**, for example) can promote variations in the receptor−ligand interactions. Further, we propose that different ligand binding conformations (*aroyl-up1* and *aroyl-up2* of **1**, for example) for the same binding pocket[64] may initiate diverse types of receptor motions for ligand-specific conformational changes in the receptor.

SUMMARY AND CONCLUSIONS

In summary, inferring the findings of extensive CB_1 receptor SAR and correlation between AAI binding affinity data and calculated binding energies, we postulated two binding conformations of **1**. It was revealed that aromatic−aromatic interactions were important for receptor binding of **1** for the aroyl ring moiety. A comprehensive conformational analysis of **1** suggested that the aroyl ring moiety could be the steric trigger important for inducing CB_1 receptor conformational change, whereas the indole ring and the morpholinyl moiety would serve as the plug important for receptor association. It appeared that differences in the nature of the ligand binding between **1** and **2** could contribute to ligand-specific conformational changes in the receptor. Detailed MD simulations to test the proposed steric trigger mechanism warrant further investigation and evaluation.

ACKNOWLEDGMENT

We wish to thank the National Institute on Drug Abuse for support for this work via grants R01-DA06312, K05-DA00182, and U24-DA12385.

REFERENCES AND NOTES

(1) Gether, U. Uncovering Molecular Mechanisms Involved in Activation of G protein-coupled Receptors. *Endocr. Rev.* **2000**, *21*, 90−113.
(2) Devane, W. A.; Dysarz, F. A., III.; Johnson, M. R.; Melvin, L. S.; Howlett, A. C. Determination and Characterization of a Cannabinoid Receptor in Rat Brain. *Mol. Pharmacol*. **1988**, *34*, 605−613.
(3) Matsuda, L. A.; Lolait, S. J.; Brownstein, M. J.; Young, A. C.; Bonner, T. I. Structure of a Cannabinoid Receptor and Functional Expression of the Cloned cDNA. *Nature* **1990**, *346*, 561−564.
(4) Munro, S.; Thomas, K. L.; Abu-Shaar, M. Molecular Characterization of a Peripheral Receptor for Cannabinoids. *Nature* **1993**, *365*, 61−65.
(5) Howlett, A. C.; Barth, F.; Bonner, T. I.; Cabral, G.; Casellas, P.; Devane, W. A.; Felder, C. C.; Herkenham, M.; Mackie, K.; Martin, B. R.; Mechoulam, R.; Pertwee. R. G. International Union of Pharmacology. XXVII. Classification of Cannabinoid Receptors. *Pharmacol. Rev.* **2002**, *54*, 161−202.

(6) Samama, P.; Cotecchia, S.; Costa, T.; Lefkowitz, R. J. A mutation-induced activated state of the beta 2-adrenergic receptor. Extending the ternary complex model. *J. Biol. Chem.* **1993**, *268*, 4625−4636.
(7) Bennett, W. S., Jr.; Steitz, T. A. Glucose-induced conformational change in yeast hexokinase. *Proc. Natl. Acad. Sci. U.S.A.* **1978**, *75*, 4848−4852.
(8) Howlett, A. C. Efficacy in CB_1 Receptor-mediated Signal Transduction. *Br. J. Pharmacol.* **2004**, *142*, 1209−1218.
(9) Song, Z. H.; Bonner, T. I. A Lysine Residue of the Cannabinoid Receptor is Critical for Receptor Recognition by Several Agonists but Not WIN55212-2. *Mol. Pharmacol.* **1996**, *49*, 891−896.
(10) Chin, C.-N.; Lucas-Lenard, J.; Abadji, V.; Kendall, D. A. Ligand Binding and Modulation of Cyclic AMP Levels Depend on the Chemical Nature of Residue 192 of the Human Cannabinoid Receptor 1. *J. Neurochem.* **1998**, *70*, 366−373.
(11) Semus, S. F.; Martin, B. R. A Computer Graphic Investigation into the Pharmacological Role of the THC-cannabinoid Phenolic Moiety. *Life Sci.* **1990**, *46*, 1781−1785.
(12) Shim, J.-Y.; Welsh, W. J.; Howlett, A. C. Homology Model of the CB_1 Cannabinoid Receptor: Sites Critical for Nonclassical Cannabinoid Agonist Interaction. *Biopolymers* **2003**, *71*, 169−189.
(13) Tao, Q.; McAllister, S. D.; Andreassi, J.; Nowell, K. W.; Cabral, G. A.; Hurst, D. P.; Bachtel, K.; Ekman, M. C.; Reggio, P. H.; Abood, M. E. Role of a Conserved Lysine Residue in the Peripheral Cannabinoid Receptor (CB2): Evidence for Subtype Specificity. *Mol. Pharmacol.* **1999**, *55*, 605−613.
(14) Bell, M. R.; D′Ambra, T. E.; Kumar, V.; Eissenstat, M. A.; Herrmann, Jr. J. L.; Wetzel, J. R.; Rosi, D.; Philion, R. E.; Daum, S. J.; Hlasta, D. J.; Kullnig, R. K.; Ackerman, J. H.; Haubrich, D. R.; Luttinger, D. A.; Baizman, E. R.; Miller, M. S.; Ward, S. J. Antinociceptive (Aminoalkyl)indoles. *J. Med. Chem.* **1991**, *34*, 1099−1110.
(15) D'Ambra, T. E.; Estep, K. G.; Bell, M. R.; Eissenstat, M. A.; Josef, K. A.; Ward, S. J.; Haycock, D. A.; Baizman, E. R.; Casiano, F. M.; Beglin, N. C.; Chippari, S. M.; Grego, J. D.; Kullnig, R. K.; Daley, G. T. Conformationally Restrained Analogues of Pravadoline: Nanomolar Potent, Enantioselective, (Aminoalkyl)indole Agonists of the Cannabinoid Receptor. *J. Med. Chem.* **1992**, *35*, 124−135.
(16) Eissenstat, M. A.; Bell, M. R.; D'Ambra, T. E.; Alexander, E. J.; Daum, S. J.; Ackerman, J. H.; Gruett, M. D.; Kumar, V.; Estep, K. G.; Olefirowicz, E. M.; Wetzel, J. R.; Alexander, M. D.; Weaver, III, J. D.; Haycock, D. A.; Luttinger, D. A.; Casiano, F. M.; Chippari, S. M.; Kuster, J. E.; Stevenson, J. I.; Ward, S. J. Aminoalkylindoles: Structure−Activity Relationships of Novel Cannabinoid Mimetics. *J. Med. Chem.* **1995**, *38*, 3094−3105.
(17) Shim, J.-Y.; Collantes, E. R.; Welsh, W. J.; Subramaniam, B.; Howlett, A. C.; Eissenstat, M. A.; Ward, S. J. Three-dimensional Quantitative Structure−activity Relationship Study of the Cannabimimetic (Aminoalkyl)indoles Using Comparative Molecular Field Analysis. *J. Med. Chem.* **1998**, *41*, 4521−4532.
(18) Wiley: J. L.; Compton, D. R.; Dai, D.; Lainton, J. A.; Phillips, M.; Huffman, J. W.; Martin, B. R. Structure−activity Relationships of Indole- and Pyrrole-derived Cannabinoids. *J. Pharmacol. Exp. Ther.* **1998**, *285*, 995−1004.
(19) Kuster, J. E.; Stevenson, J. I.; Ward, S. J.; D'Ambra, T. E.; Haycock, D. A. Aminoalkylindole Binding in Rat Cerebellum: Selective Displacement by Natural and Synthetic Cannabinoids. *J. Pharmacol. Exp. Ther.* **1993**, *264*, 1352−1363.
(20) Song, Z. H.; Slowey, C. A.; Hurst, D. P.; Reggio, P. H. The Difference between the CB(1) and CB(2) Cannabinoid Receptors at Position 5.46 is Crucial for the Selectivity of WIN55212-2 for CB(2). *Mol. Pharmacol.* **1999**, *56*, 834−840.
(21) Bramblett, R. D.; Panu, A. M.; Ballesteros, J. A.; Reggio, P. H. Construction of a 3D Model of the Cannabinoid CB_1 Receptor: Determination of Helix Ends and Helix Orientation. *Life Sci.* **1995**, *56*, 1971−1982.
(22) McAllister, S. D.; Rizvi, G.; Anavi-Goffer, S.; Hurst, D. P.; Barnett-Norris, J.; Lynch, D. L.; Reggio, P. H.; Abood, M. E. An Aromatic Microdomain at the Cannabinoid CB_1 Receptor Constitutes an Agonist/inverse Agonist Binding Region. *J. Med. Chem.* **2003**, *46*, 5139−5152.
(23) Razdan, R. K. Structure−activity Relationships in Cannabinoids. *Pharmacol. Rev.* **1986**, *38*, 75−149.
(24) Howlett, A. C.; Johnson, M. R.; Melvin, L. S.; Milne, G. M. Nonclassical Cannabinoid Analgetics Inhibit Adenylate Cyclase: Development of a Cannabinoid Receptor Model. *Mol. Pharmacol.* **1988**, *33*, 297−302.
(25) Mechoulam, R.; Edery, H. Structure Activity Relationships in the Cannabinoid Series. In *Marijuana Chemistry, Pharmacology, Metabolism and Clinical Effects*; Mechoulam, R., Ed.; Academic: New York, 1973; pp 101−136.
(26) Melvin, L. S.; Milne, G. M.; Johnson, M. R.; Subramaniam, B.; Wilken, G. H.; Howlett, A. C. Structure−activity Relationships for Cannabinoid Receptor-binding and Analgesic Activity: Studies of Bicyclic Cannabinoid Analogues. *Mol. Pharmacol.* **1993**, *44*, 1008−1015.
(27) Busch-Petersen, J.; Hill, W. A.; Fan, P.; Khanolkar, A.; Xie, X. Q.; Tius, M. A.; Makriyannis, A. Unsaturated Side Chain β-11-Hydroxy-hexahydrocannabinol Analogs. *J. Med. Chem.* **1996**, *39*, 3790−3796.
(28) Huffman, J. W.; Liddle, J.; Duncan, S. G., Jr.; Yu, S.; Martin, B. R.; Wiley, J. L. Synthesis and Pharmacology of the Isomeric Methylheptyl-Δ^8-tetrahydrocannabinols. *Bioorg. Med. Chem.* **1998**, *6*, 2383−2396.
(29) Martin, B. R.; Jefferson, R.; Winckler, R.; Wiley, J. L.; Huffman, J. W.; Crocker, P. J.; Saha, B.; Razdan, R. K. Manipulation of the Tetrahydrocannabinol Side Chain Delineates Agonists, Partial Agonists, and Antagonists. *J. Pharmacol. Exp. Ther.* **1999**, *290*, 1065−1079.
(30) Shim, J.-Y.; Howlett, A. C. Steric Trigger as a Mechanism for CB_1 Cannabinoid Receptor Activation. *J. Chem. Inf. Comput. Sci.* **2004**, *44*, 1466−1476.
(31) Maple, J. R.; Hwang, M.-J.; Stockfisch, T. P.; Dinur, U.; Waldman, M.; Ewig, C. S.; Hagler, A. T. Derivation of Class II Force Fields. I. Methology and Quantum Force Field for the Alkyl Functional Group and Alkane Molecules. *J. Comput. Chem.* **1994**, *15*, 162−182.
(32) Press: W. H.; Teukolsky, S. A.; Vetterling, W. T.; Flanery, B. P. *Numerical Recipes − The Art of Scientific Computing*; Cambridge University Press: Cambridge, 1993; pp 420−424.
(33) Ding, H. Q.; Karasawa, N.; Goddard, W. A., III. Atomic Level Simulations on a Million Particles: the Cell Multipole Method for Coulomb and London Nonbond Interactions. *J. Chem. Phys.* **1992**, *97*, 4309−4315.
(34) Palczewski, K.; Kumasaka, T.; Hori, T.; Behnke, C. A.; Motoshima, H.; Fox, B. A.; Le Trong, I.; Teller, D. C.; Okada, T.; Stenkamp, R. E.; Yamamoto, M.; Miyano, M. Crystal Structure of Rhodopsin: A G. Protein-coupled Receptor. *Science* **2000**, *289*, 739−745.
(35) Halgren, T. A. Merck Molecular Force Field. I. Basis, Form, Scope, Parameterization, and Performance of MMFF94. *J. Comput. Chem.* **1996**, *17*, 490−519.
(36) Dewar, M. J. S.; Zoebisch, E. G.; Healy, E. F.; Stewart, J. J. P. AM1: A New General Purpose Quantum Mechanical Molecular Model. *J. Am. Chem. Soc.* **1985**, *107*, 3902−3909.
(37) Hehre, W. J.; Radom, L.; Schleyer, P. v. R.; Pople, J. A. *Ab Initio Molecular Orbital Theory*; Wiley: New York, 1986.
(38) Swope, W. C.; Andersen, H. C.; Berens, P. H.; Wilson, K. R. A Computer Simulation Method for the Calculation of Equilibrium Constants for the Formation of Physical Clusters of Molecules: Application to Small Water Clusters. *J. Chem. Phys.* **1982**, *76*, 637−649.
(39) Tuckerman, M.; Berne, B. J.; Martyna, G. J. Reversible Multiple Time Scale Molecular Dynamics. *J. Chem. Phys.* **1992**, *97*, 1990−2001.
(40) Tsuzuki, S.; Honda, K.; Uchimaru, T.; Mikami, M.; Tanabe, K. Origin of Attraction and Directionality of the π/π Interaction: Model Chemistry Calculations of Benzene Dimer Interaction. *J. Am. Chem. Soc.* **2002**, *124*, 104−112.
(41) Sinnokrot, M. O.; Valeev, E. F.; Sherrill, C. D. Estimates of the Ab Initio Limit for π-π Interactions: the Benzene Dimer. *J. Am. Chem. Soc.* **2002**, *124*, 10887−10893.
(42) McGaughey, G. B.; Gagné, M., Rappé, A. K. π-Stacking Interactions. Alive and Well in Proteins. *J. Biol. Chem.* **1998**, *273*, 15458−15463.
(43) Tao, Q.; Abood, M. E. Mutation of a Highly Conserved Aspartate Rresidue in the Second Transmembrane Domain of the Cannabinoid Receptors, CB_1 and CB_2, Disrupts G-protein Coupling. *J. Pharmacol. Exp. Ther.* **1998**, *285*, 651−658.
(44) Simpson, M. M.; Ballesteros, J. A.; Chiappa, V.; Chen, J.; Suehiro, M.; Hartman, D. S.; Godel, T.; Snyder, L. A.; Sakmar, T. P.; Javitch, J. A. Dopamine D4/D2 Receptor Selectivity is Determined by a Divergent Aromatic Microdomain Contained within the Second, Third, and Seventh Membrane-spanning Segments. *Mol. Pharmacol.* **1999**, *56*, 1116−1126.
(45) Govaerts, C.; Bondue, A.; Springael, J. Y.; Olivella, M.; Deupi, X.; Le Poul E.; Wodak, S. J.; Parmentier, M.; Pardo, L.; Blanpain, C. Activation of CCR5 by Chemokines Involves an Aromatic Cluster between Transmembrane Helices 2 and 3. *J. Biol. Chem.* **2003**, *278*, 1892−1903.
(46) (a) Shire, D.; Calandra, B.; Delpech, M.; Dumont, X.; Kaghad, M.; Le Fur, G.; Caput, D.; Ferrara, P. Structural Features of the Central Cannabinoid CB1 Receptor Iinvolved in the Binding of the Specific CB1 Antagonist SR 141716A. *J. Biol. Chem.* **1996**, *271*, 6941−6946. (b) Shire, D.; Calandra, B.; Bouaboula, M.; Barth, F.; Rinaldi-Carmona, M.; Casellas, P.; Ferrara, P. Cannabinoid Receptor Interactions with the Antagonists SR 141716A and SR 144528. *Life Sci.* **1999**, *65*, 627−635.
(47) McAllister, S. D.; Tao, Q.; Barnett-Norris, J.; Buehner, K.; Hurst, D. P.; Guarnieri, F.; Reggio, P. H.; Nowell Harmon, K. W.; Cabral, G. A.; Abood, M. E. A Critical Role for a Tyrosine Residue in the

Cannabinoid Receptors for Ligand Recognition. *Biochem. Pharmacol*. **2002**, *63*, 2121−2136.
(48) Shieh, T.; Han, M.; Sakmar, T. P.; Smith, S. O. The Steric Trigger in Rhodopsin Activation. *J. Mol. Biol*. **1997**, *269*, 373−384.
(49) Swaminath, G.; Xiang, Y.; Lee, T. W.; Steenhuis, J.; Parnot, C.; Kobilka, B. K. Sequential Binding of Agonists to the β_2 Adrenoceptor. Kinetic Evidence for Intermediate Conformational States. *J. Biol. Chem*. **2004**, *279*, 686−691.
(50) Huffman, J. W.; Dai, D.; Martin, B. R.; Compton, D. R. Design, Synthesis and Pharmacology of Cannabimimetic Indoles. *Bioorg. Med. Chem. Lett*. **1994**, *4*, 563−566.
(51) Xie, X.-Q.; Eissenstat, M.; Makriyannis, A. Common Cannabimimetic Pharmacophoric Requirements between Aminoalkylindoles and Classical Cannabinoids. *Life Sci*. **1995**, *56*, 1963−1970.
(52) Shim, J.-Y.; Collantes, E. R.; Welsh, W. J.; Howlett, A. C. United Pharmacophoric Model for Cannabinoids and Aminoalkylindoles Derived from Molecular Superimposition of CB_1 Cannabinoid Receptor Agonists CP55244 and WIN55212-2. In *Rational Drug Design Symposium Series*; Parril, A. L., Reddy, M. R., Eds.; American Chemical Society: Washington, DC, 1999; pp 165−184.
(53) Huffman, J. W.; Lu, J.; Dai, D.; Kitaygorodskiy, A.; Wiley, J. L.; Martin, B. R. Synthesis and Pharmacology of a Hybrid Cannabinoid. *Bioorg. Med. Chem*. **2000**, *8*, 439−447.
(54) Reggio, P. H.; Basu-Dutt, S.; Barnett-Norris, J.; Castro, M. T.; Hurst, D. P.; Seltzman, H. H.; Roche, M. J.; Gilliam, A. F.; Thomas, B. F.; Stevenson, L. A.; Pertwee, R. G.; Abood, M. E. The Bioactive Conformation of Aminoalkylindoles at the Cannabinoid CB_1 and CB_2 Receptors: Insights Gained from (E)- and (Z)-Naphthylidene Indenes. *J. Med. Chem*. **1998**, *41*, 5177−5187.
(55) Kumar, V.; Alexander, M. D.; Bell, M. R.; Eissenstat, M. A.; Casiano, F. M.; Chippari, S. M.; Haycock, D. A.; Luttinger, D. A.; Kuster, J. E.; Miller, M. S.; Stevenson, J. I.; Ward, S. J. Morpholinoalkylindenes as Antinociceptive Agents: Novel Cannabinoid Receptor Agonists. *Bioorg. Med. Chem. Lett*. **1995**, *4*, 381−386.
(56) Chin, C.-N.; Murphy, J. W.; Huffman, J. W.; Kendall, D. A. The Third Transmembrane Helix of the Cannabinoid Receptor Plays a Role in the Selectivity of Aminoalkylindoles for CB2, Peripheral Cannabinoid Receptor. *J. Pharmacol. Exp. Therap*. **1999**, *291*, 837−844.
(57) Saam, J.; Tajkhorshid, E.; Hayashi, S.; Schulten, K. Molecular Dynamics Investigation of Primary Photoinduced Events in the Activation of Rhodopsin. *Biophys. J*. **2002**, *83*, 3097−3112.
(58) Shi, L.; Javitch J. A. The Second Extracellular Loop of the Dopamine D2 Receptor Lines the Binding-site Crevice. *Proc. Natl. Acad. Sci. U.S.A.* **2004**, *101*, 440−445.
(59) Ghanouni, P.; Steenhuis, J. J.; Farrens, D. L.; Kobilka, B. K. Agonist-induced Conformational Changes in the G-Protein-Coupling Domain of the β_2 Adrenergic Receptor. *Proc. Natl. Acad. Sci. U. S. A*. **2001**, *98*, 5997−6002.
(60) Ghanouni, P.; Gryczynski, Z.; Steenhuis, J. J.; Lee, T. W.; Farrens, D. L.; Lakowicz, J. R.; Kobilka, B. K. Functionally Different Agonists Induce Distinct Conformations in the G Protein Coupling Domain of the β_2 Adrenergic Receptor. *J. Biol. Chem*. **2001**, *276*, 24433−24436.
(61) Kenakin, T.; Onaran, O. The Ligand Paradox between Affinity and Efficacy: Can You Be There and Not Make a Difference? *Trends. Pharmacol. Sci*. **2002**, *23*, 275−280.
(62) Sealfon, S. C.; Chi, L.; Ebersole, B. J.; Rodic, V.; Zhang, D.; Ballesteros, J. A.; Weinstein, H. Related Contribution of Specific Helix 2 and 7 Residues to Conformational Activation of the Serotonin 5-HT2A Receptor. *J. Biol. Chem*. **1995**, *270*, 16683−16688.
(63) Klco, J. M.; Wiegand, C. B.; Narzinski, K.; Baranski, T. J. Essential Role for the Second Extracellular Loop in C5a Receptor Activation. *Nat. Struct. Mol. Biol.* **2005**, *12*, 320−326.
(64) Ma, B.; Shatsky, M.; Wolfson, H. J.; Nussinov, R. Multiple Diverse Ligands Binding at a Single Protein Site: A Matter of Pre-Existing Populations. *Protein Sci.* **2002**, *11*, 184−197.

CI0504824